

Measurements of the Neutron Cross Sections of Hydrogen and Deuterium in H₂O-D₂O Mixtures Using the Deep Inelastic Neutron-Scattering Technique

J. J. Blostein, L. A. Rodríguez Palomino, and J. Dawidowski*

Consejo Nacional de Investigaciones Científicas y Técnicas, Centro Atómico Bariloche and Instituto Balseiro, Comisión Nacional de Energía Atómica, Universidad Nacional de Cuyo, (8400) Bariloche, Argentina

(Received 11 September 2008; published 2 March 2009)

We investigated the neutron cross sections of hydrogen and deuterium by means of the deep inelastic neutron-scattering technique in H₂O-D₂O mixtures. The interest in this work was to examine the anomalous behavior in the hydrogen neutron cross section reported in the past in similar experiments that raised a yet unsettled controversy. The measurements were made at the Bariloche pulsed neutron source (Argentina) in pure H₂O and D₂O, with mixtures of molar concentrations of deuterium of $x_D = 0.3$ and 0.4, at room temperature, under the same experimental conditions as the former experiments. The results are in good agreement with the standard cross sections and are incompatible with the anomalies pointed out.

DOI: 10.1103/PhysRevLett.102.097401

PACS numbers: 78.70.Nx, 28.20.Cz, 61.05.fd

In this Letter, we report on recent experiments of deep inelastic neutron scattering (DINS) on light water and heavy water mixtures aiming to elucidate the controversial issue originating with the publication of Ref. [1] that still remains unsettled. In the mentioned work (performed with the DINS technique), a hydrogen neutron cross section significantly lower than the tabulated values commonly accepted in neutron physics was reported. Subsequent DINS experiments by the same authors supported their previous report [2,3], while results from different neutron techniques did not confirm them [4–7]. Some authors ascribed it to the fact that these experiments were done in scattering conditions essentially different from DINS, thus preventing a direct comparison of results. This generated divergent positions [8] that extended to the correctness of the method employed to interpret the data [9–12] and led to conflicting theoretical interpretations (exhaustively reviewed by Colognesi in Ref. [13]), without a consensus about the fundamental grounds.

A common feature of the growing number of unexpected experimental results is that the studied materials contain hydrogen in their composition, and the anomalous figures are always a resultant of the analysis of the hydrogen signal in the observed profiles. In addition, it must be remarked that hydrogen analysis in DINS experiments is a particularly delicate task [9]. This is so because the contribution to the DINS signal of hydrogen is due to the fastest neutrons of the incident spectrum, with energies ranging from the epithermal region up to hundreds of eV. Measurements in this energy region are especially involved due to the severe dead time [14] and efficiency corrections that must be performed when a detector is placed in the direct beam. This consideration is particularly relevant in the determination of the incident spectrum, one of the crucial magnitudes to describe the DINS spectra [15], that has to be known in a wide range of energies. For this reason, the

different views about the method that has to be employed in the DINS data treatment lead to more disagreeing results for hydrogen than for any other atom [9].

The key to solve this problem is to elucidate unequivocally the relationship between the measured and the calculated magnitudes. A necessary step to do this is an exhaustive study of the parameters that take part in the neutron Compton profiles [15]. Thus, prior to the measurements, a careful characterization of the detector bank efficiency and the incident spectrum as well as the transmission of the employed resonant filter has to be performed. In order to meet the above-mentioned premises, we set out an experimental program that comprised the following stages: (i) building a new detector bank [16], (ii) development of data processing procedures [15] and related software [17], (iii) optimization of the detection system (shieldings, electronic parameters), and (iv) characterization of the spectrometer parameters, i.e., incident neutron spectrum, background, detectors, and electronic dead-time, filter thickness, and flight paths.

The experiments described in this Letter were performed at the Bariloche pulsed neutron source facility (LINAC), Argentina. The accelerator, that produces 25 MeV electron pulses of 1 μ s width, operated at a frequency of 100 Hz and at a mean electron current of 24 μ A, producing fast neutrons that were moderated in a 40 mm thick polyethylene slab. A cadmium sheet was placed in the neutron beam to avoid frame overlap by absorbing thermal neutrons. The epithermal neutron beam was collimated up to 5.08 cm diameter at the sample position. The detector bank consists of 10 cylindrical ³He proportional counters filled at a pressure of 10 bar arranged in a decagonal geometry, subtending a mean angle of 70° in the forward direction with respect to the incident beam as described in Ref. [16]. This kind of detector was preferred because of its lower gamma efficiency compared with that of the ⁶Li scintillators. The

detectors were covered with cadmium cylinders to minimize the background due to thermal neutrons. The flight-path lengths were 488.1 (source-sample) and 49.4 cm (sample-detector), respectively. The time-of-flight spectra were recorded in 4096 channels, $2 \mu\text{s}$ width each. Measurements were possible starting from $50 \mu\text{s}$ after the LINAC pulse due to electronic perturbations on the baseline caused by the intense bremsstrahlung radiation. An independent detector placed near the neutron source was employed as a monitor, which served to normalize the spectra. The filter was a cylindrical gold foil 0.0535 mm thick whose thickness was determined by neutron transmission and checked by weight. It was mounted on an aluminum cylinder placed in a remote-controlled movable structure, devised to perform “filter-in” and “filter-out” alternative measurements every 10 minutes. The filter was placed coaxially with the incident beam, and its diameter was greater than that of the incident beam, in order to mainly absorb neutrons scattered towards the detector bank. In such a way we minimize a filter-dependent background that otherwise could have an important contribution to the spectra. In addition, we avoided placing additional shielding pieces near the detectors, given that it could increase the effective scattering angle by in-scattering processes. In the filter-out position, an aluminum cylinder was placed as a dummy filter. The samples were prepared in a dry atmosphere starting from reactor-quality D_2O (0.9987 M) and nano pure H_2O . The measurements were performed on four different systems at room temperature. The deuterium molar concentrations of the mixtures were $x_{\text{D}} = 0$ (light water), 0.3, 0.4, and 1 (heavy water). A coin-shaped aluminum can 2 mm thick and 5.08 cm diameter was employed as a sample container.

The details of the characterization of the experimental bank will be published elsewhere, so only a brief summary is given here. In the first step, we determined the incident neutron spectrum. For this purpose, a ^3He proportional counter was placed in the direct beam position. The detector efficiency had been previously checked by measuring its transmission and comparing it with the one calculated by the transmission of a 10-bar gas cylinder of ^3He . The measured spectrum was thus corrected by efficiency. Also, corrections due to background contribution and dead time of the system [14] were performed and verified by measurements at different beam diameters. The energy scale was determined by the time-of-flight method and calibrated by observing known lines in the transmitted beam through resonant filters. The background was measured by displacing the detector off the direct beam, checked at particular energy regions by comparison with the transmitted beam through thick resonant filters, and also verified with a beamstop placed in the direct beam. The incident spectrum measurement was also checked at different flight paths.

The DINS detector bank efficiency was determined by the ratio between the spectrum of the scattered neutrons by a Pb sample and the incident neutron spectrum. After

correcting the spectrum of Pb by background, it was corrected by multiple scattering and beam attenuation with the Monte Carlo procedure below described. Since the detector efficiency function is a required input data of the Monte Carlo code, its determination was performed by means of a recursive method. In the first run, the zero-order input efficiency was the experimental Pb spectrum divided by the incident spectrum. The Pb spectrum corrected by attenuation and multiple scattering after the first run allowed us to calculate a new efficiency for the second run. The recursive process converged after three runs and was checked with lead samples of different sizes.

Monte Carlo simulations were performed along the lines described in Ref. [18]. Neutron histories randomly generated are followed individually. At each step, the flight path is randomly obtained from a distribution governed by the total cross section as a function of the neutron energy taken from experimental data [5,19]. The distribution is biased in order that the neutron never leaves the sample. The energy after each scattering process is determined by a gas mixture of H, D, and O with the effective temperatures previously checked by neutron transmission experiments [20]. The bound-atom cross sections were taken from the standard tables (see, e.g., Ref. [21]).

In Fig. 1, we show the measured neutron Compton profile of the $x_{\text{D}} = 0.4$ mixture, for which the largest statistics was collected. The data processing procedure performed consists in computing the difference of each (monitor normalized) filter-in and filter-out spectra. The mean value and its statistical error were calculated for each channel. The data shown in Fig. 1 involved the measurement of 540 couples during a period of 1 month. Time channels were grouped into bins of 4 channels each. The result is compared with the Monte Carlo run obtained after computing 1 500 000 histories. A scale factor that links the experimental units with the Monte Carlo results was computed by least squares, thus allowing us to represent both

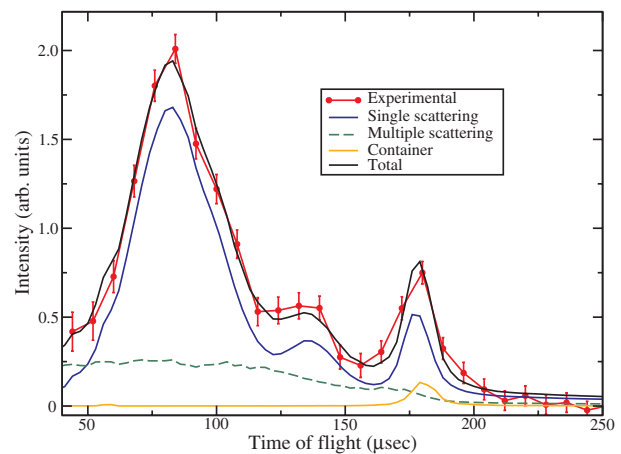


FIG. 1 (color online). Measured neutron Compton profile for the mixtures $x_{\text{D}} = 0.4$. The results of the Monte Carlo simulations show the single scattering contribution, the multiple scattering, the container contribution, and the total scattering.

results in the same scale. We proceeded similarly with the rest of the measurements.

The Monte Carlo results allow a correction procedure of the experimental data by multiple scattering, beam attenuation, container contribution, and detector efficiency effects. The procedure we applied is based on Ref. [17]. In Fig. 2, we show the corrected data results for the four samples, where the arbitrary vertical scale is expressed in experimental units, which is the same for the four samples.

To determine the peak intensities, we proceeded in the following way. First, we fitted a global constant that links the experimental scale with the theoretical profiles employing a theoretical expression of the neutron Compton profile [15]

$$c(t) = A \int_{E_0^{\text{inf}}}^{+\infty} dE_0 E^{3/2} \Phi(E_0) \sigma(E_0, E, \theta) [1 - e^{-nT\sigma_F(E)}], \quad (1)$$

where E_0 and E are the incident and scattered neutron energies, respectively, θ is the scattering angle,

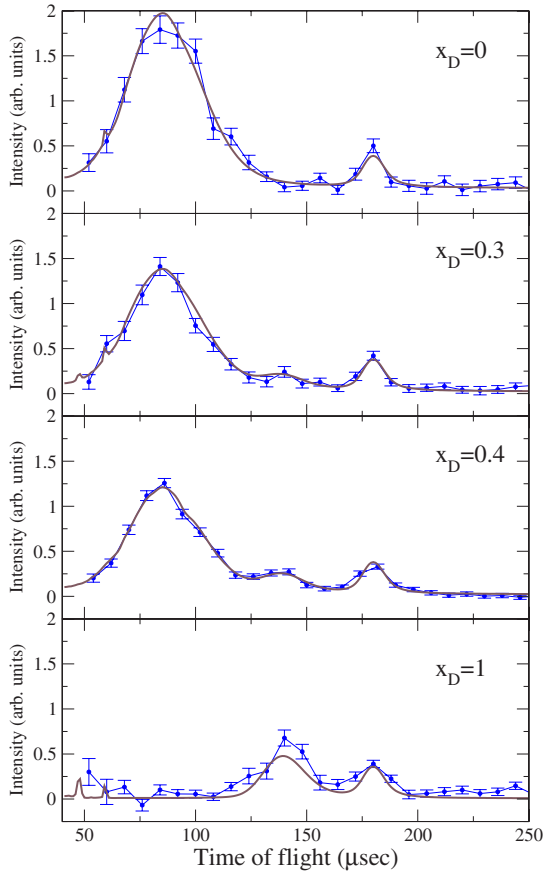


FIG. 2 (color online). Experimental neutron Compton profiles of pure H_2O ($x_D = 0$) and the mixtures $x_D = 0.3$, $x_D = 0.4$, and pure D_2O ($x_D = 1$), corrected by multiple scattering, beam attenuation, and detector efficiency. The results are compared with the theoretical Compton profiles calculated by Eq. (1) where the parameter A was simultaneously fitted for the four spectra.

$\sigma(E_0, E, \theta)$ is the sample double-differential cross section, $\Phi(E_0)$ is the incident neutron energy spectrum, and A is the instrumental constant to be determined. The term between brackets is the absorption probability of the resonant filter, characterized by a number density n , a thickness T , and a total cross section $\sigma_F(E)$. In order to describe the observed neutron Compton profiles, we employed the function $\sigma(E_0, E, \theta)$ of a mixture of H, D, and O gases with the previously mentioned effective temperatures

$$\begin{aligned} \sigma(E_0, E, \theta) = & \sqrt{\frac{E}{E_0}} [2(1 - x_D) \sigma_{b,H} s_H(E_0, E, \theta) \\ & + 2x_D \sigma_{b,D} s_D(E_0, E, \theta) \\ & + \sigma_{b,O} s_O(E_0, E, \theta)], \end{aligned} \quad (2)$$

where the effects of the HDO molecule formation were neglected, the functions s_X are the gas scattering functions for the atom X , and $\sigma_{b,X}$ are the tabulated bound-atom cross sections. The instrumental constant A was determined by simultaneous least-squares fitting the four curves to the experimental data. The result of such fitting (shown in Fig. 2) provides a link between the experimental units and the theoretical calculations.

In the second step, we allowed for the variation of the individual peak intensities by fitting the expression

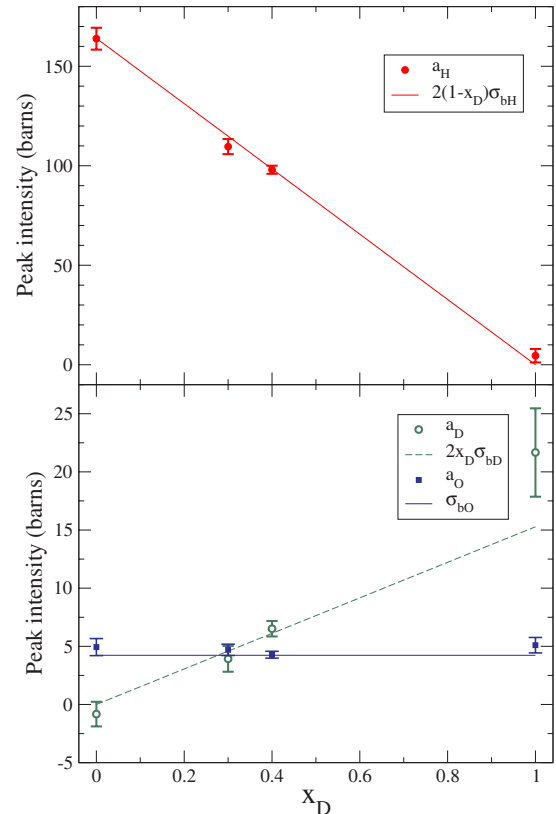


FIG. 3 (color online). Experimental peak intensities of the obtained Compton profiles of the four samples, compared with the theoretical values.

$$c(t) = a_H c_H(t) + a_D c_D(t) + a_O c_O(t) \quad (3)$$

to the experimental data shown in Fig. 2, where $c_X(t)$ is the Compton profile for atom X , calculated as in Eq. (1) by replacing the $\sigma(E_0, E, \theta)$ by $\sqrt{E/E_0} s_X(E_0, E, \theta)$. Therefore, the parameters a_H , a_D , and a_O are the sought intensities expressed in barns. The fitted values for each sample are shown in Fig. 3 compared with the intensities resulting from the theoretical expression (2). A good agreement is observed between the hydrogen intensities and the theoretically predicted expression $2(1 - x_D)\sigma_{b,H}$, and the same occurs between the deuterium intensities and the value $2x_D\sigma_{b,D}$ and the oxygen intensity and $\sigma_{b,O}$. It should be noted that the sample $x_D = 0.4$ has the best experimental statistics of the four studied samples, which is manifested in the smaller error bars in Fig. 3, whereas the pure heavy water data ($x_D = 1$) has the lowest statistics, due to the shorter time of measurement and the smaller scattering power of the sample.

The results presented in this Letter are fully compatible with the commonly accepted tabulated values of neutron cross sections of hydrogen, deuterium, and oxygen. To obtain these results, a complete characterization and data treatment process of the DINS experiment was essential. The process involved different stages starting from the construction of the detector bank, the characterization of the experimental parameters, and the development of the data processing tools. A special effort was devoted to the determination of the magnitudes that play a central role in the calculation of the Compton profiles [Eq. (1)], such as the incident spectrum, the filter thickness, and the detector bank efficiency. In this task it was essential to develop the tools for multiple scattering, attenuation, and efficiency corrections [17], as had been previously done in relation to different neutron techniques [18,22].

We chose to concentrate our efforts in the measurement of the sample $x_D = 0.4$ in which an anomalous decrement of about 30% in the cross section had been reported [1]. In the present work, we show that the value of the intensity of the H peak fully agrees with the value $2(1 - x_D)\sigma_{b,H}$ within the 2% error as shown in Fig. 3, where $\sigma_{b,H}$ is taken from reference tables [21]. A good agreement is also found for the D and O peaks. The rest of the examined mixtures, while not comparable in the quality of statistics, clearly confirm a full agreement with the standard data.

The present results are in line with former works that did not show anomalous values in the H cross section [4–7], whose validity was questioned by arguing that they were obtained at different experimental situations [8,23]. The results here presented rule out the existence of the anomalous neutron cross sections referred to above.

We gratefully acknowledge ANPCyT (Projects No. PICT 25963/34534), CONICET (Project No. PIP

5249), and Universidad de Cuyo (Project No. 06/C240) for financial support. We are especially grateful to L. Capararo, M. Schneebeli, and P. D'Avanzo for technical support.

*javier@cab.cnea.gov.ar

- [1] C. A. Chatzidimitriou-Dreismann, T. Abdul Redah, R.M.F. Streffer, and J. Mayers, Phys. Rev. Lett. **79**, 2839 (1997).
- [2] C. A. Chatzidimitriou-Dreismann, T. Abdul-Redah, and J. Mayers, Physica (Amsterdam) **315B**, 281 (2002).
- [3] C. A. Chatzidimitriou-Dreismann, T. Abdul-Redah, and M. Krzystyniak, Phys. Rev. B **72**, 054123 (2005).
- [4] A. Ioffe, M. Arif, D. L. Jacobson, and F. Mezei, Phys. Rev. Lett. **82**, 2322 (1999).
- [5] J. J. Blostein, J. Dawidowski, S. A. Ibáñez, and J. R. Granada, Phys. Rev. Lett. **90**, 105302 (2003).
- [6] R. Moreh, R. C. Block, Y. Danon, and M. Neuman, Phys. Rev. Lett. **94**, 185301 (2005).
- [7] R. Moreh, R. C. Block, Y. Danon, and M. Neuman, Phys. Rev. Lett. **96**, 055302 (2006).
- [8] E. B. Karlsson and J. Mayers, Phys. Rev. Lett. **92**, 249601 (2004); J. J. Blostein, J. Dawidowski, and J. R. Granada, Phys. Rev. Lett. **92**, 249602 (2004).
- [9] J. J. Blostein, J. Dawidowski, and J. R. Granada, Physica (Amsterdam) **304B**, 357 (2001); **334B**, 257 (2003).
- [10] J. Mayers and T. Abdul-Redah, J. Phys. Condens. Matter **16**, 4811 (2004).
- [11] M. Krzystyniak and C. A. Chatzidimitriou-Dreismann, Phys. Rev. B **72**, 174117 (2005).
- [12] J. J. Blostein, J. Dawidowski, and J. R. Granada, arXiv: physics/0601221v1.
- [13] D. Colognesi, Physica (Amsterdam) **398B**, 89 (2007).
- [14] G. J. Cuello, P. J. Prado, and J. Dawidowski, Nucl. Instrum. Methods Phys. Res., Sect. A **325**, 309 (1993).
- [15] J. J. Blostein, J. Dawidowski, and J. R. Granada, Phys. Rev. B **71**, 054105 (2005).
- [16] L. A. Rodríguez Palomino, J. J. Blostein, J. Dawidowski, and G. J. Cuello, JINST **3**, P06005 (2008).
- [17] J. Dawidowski, J. J. Blostein, and J. R. Granada, JINST **1**, P06002 (2006).
- [18] L. A. Rodríguez Palomino, J. Dawidowski, J. J. Blostein, and G. J. Cuello, Nucl. Instrum. Methods Phys. Res., Sect. B **258**, 453 (2007).
- [19] J. R. Granada, V. H. Gillette, and R. E. Mayer, Phys. Rev. A **36**, 5594 (1987).
- [20] J. J. Blostein, J. Dawidowski, and J. R. Granada, Physica (Amsterdam) **385B–386B**, 69 (2006).
- [21] V. F. Sears, Neutron News **3**, 26 (1992).
- [22] J. Dawidowski, F. J. Bermejo, and J. R. Granada, Phys. Rev. B **58**, 706 (1998).
- [23] C. A. Chatzidimitriou-Dreismann, T. Abdul Redah, R.M.F. Streffer, and B. Hessmo, Phys. Rev. Lett. **84**, 2036 (2000); A. Ioffe, M. Arif, D. L. Jacobson, and F. Mezei, Phys. Rev. Lett. **84**, 2037 (2000).